Unobtrusive interferometer tracking by path length oscillation for multidimensional spectroscopy

Kevin F. Lee, Adeline Bonvalet, Patrick Nuernberger, Manuel Joffre

Unobtrusive interferometer tracking by path length oscillation for multidimensional spectroscopy

Kevin F. Lee, Adeline Bonvalet, Patrick Nuernberger and Manuel Joffre*

Laboratoire d'Optique et Biosciences, Ecole Polytechnique
Centre National de la Recherche Scientifique, 91128 Palaiseau, France
Institut National de la Santé et de la Recherche Médicale, U696, 91128 Palaiseau, France
*manuel.joffre@polytechnique.edu

Abstract: We track the path difference between interferometer arms with few-nanometer accuracy without adding optics to the beam path. We measure the interference of a helium-neon beam that copropagates through the interferometer with midinfrared pulses used for multidimensional spectroscopy. This can indicate motion, but not direction. By oscillating the path length of one arm with a mirror on a piezoelectric stack and monitoring the oscillations of the recombined helium-neon beam, the direction can be calculated, and the path delay can be continuously tracked.

OCIS codes: (120.3180) Interferometry; (120.5050) Phase measurement; (300.6240) Spectroscopy, coherent transient; (300.6300) Spectroscopy, Fourier transforms; (300.6340) Spectroscopy, infrared; (300.6420) Spectroscopy, nonlinear.

References and links

1. A. A. Michelson, "The relative motion of the Earth and the Luminiferous ether," Am. J. Sci. **22**, 120–129 (1881).
2. B. Abbott *et al*. (LIGO Scientific Collaboration), "Search for Gravitational-Wave Bursts from Soft Gamma Repeaters," Phys. Rev. Lett. **101**, 211102 (2008).
3. D. M. Jonas, "Two-Dimensional Femtosecond Spectroscopy," Annu. Rev. Phys. Chem. **54,** 425–463 (2003).
4. L. P. DeFlores, R. A. Nicodemus, and A. Tokmakoff, "Two-dimensional Fourier transform spectroscopy in the pump-probe geometry," Opt. Lett. **32**, 2966–2968 (2007).
5. M. M. Salour and C. Cohen-Tannoudji, "Observation of Ramsey's Interference Fringes in the Profile of Doppler-Free Two-Photon Resonances," Phys. Rev. Lett. **38**, 757–760 (1977).
6. N. F. Scherer, R. J. Carlson, A. Matro, M. Du, A. J. Ruggiero, V. Romero-Rochin, J. A. Cina, G. R. Fleming, and S. A. Rice, "Fluorescence-detected wave packet interferometry: Time resolved molecular spectroscopy with sequences of femtosecond phase-locked pulses," J. Chem. Phys. **95**, 1487–1511 (1991).
7. T. Zhang, C. Borca, X. Li, and S. Cundiff, "Optical two-dimensional Fourier transform spectroscopy with active interferometric stabilization," Opt. Express **13**, 7432–7441 (2005).
8. C. J. Buchenauer and A. R. Jacobson, "Quadrature interferometer for plasma density measurements," Rev. Sci. Instrum. **48**, 769–774 (1977).
9. M. U. Wehner, M. H. Ulm, and M. Wegener, "Scanning interferometer stabilized by use of Pancharatnam's phase," Opt. Lett. **22**, 1455–1457 (1997).
10. S. Pancharatnam, "Generalized Theory of Interference and its Applications," Proc. Indian Acad. Sci. Sect. A **44**, 247–262 (1956).
11. N. Belabas and M. Joffre, "Visible-infrared two-dimensional Fourier-transform spectroscopy," Opt. Lett. **27**, 2043–2045 (2002).
12. M. Winter, M. Wollenhaupt, and T. Baumert, "Coherent matter waves for ultrafast laser pulse characterization," Opt. Commun. **264**, 285 – 292 (2006).
13. E. H. G. Backus, S. Garrett-Roe, and P. Hamm, "Phasing problem of heterodyne-detected two-dimensional infrared spectroscopy," Opt. Lett. **33**, 2665–2667 (2008).
14. A. D. Bristow, D. Karaiskaj, X. Dai, and S. T. Cundiff, "All-optical retrieval of the global phase for two-dimensional Fourier-transform spectroscopy," Opt. Express **16**, 18017–18027 (2008).
15. A. L. Besse and J. G. Kelley, "Interferometer for Shock Tube," Rev. Sci. Instrum. **37**, 1497–1499 (1966).
16. V. Volkov, R. Shanz, and P. Hamm, "Active phase stabilization in Fourier-transform two-dimensional infrared spectroscopy," Opt. Lett. **30**, 2010–2012 (2005).

#111806 - $15.00 USD Received 26 May 2009; revised 24 Jun 2009; accepted 1 Jul 2009; published 7 Jul 2009

17. G. D. Goodno, G. Dadusc, and R. J. D. Miller, "Ultrafast heterodyne-detected transient-grating spectroscopy using diffractive optics," J. Opt. Soc. Am. B **15**, 1791–1794 (1998).
18. A. A. Maznev, K. A. Nelson, and J. Rogers, "Optical heterodyne detection of laser-induced gratings," Opt. Lett. **23**, 1319–1321 (1998).
19. S.-H. Shim, D. B. Strasfeld, Y. L. Ling, and M. T. Zanni, "Automated 2D IR spectroscopy using a mid-IR pulse shaper and application of this technology to the human islet amyloid polypeptide," Proc. Natl. Acad. Sci. USA **104**, 14197–14202 (2007).
20. K. Gundogdu, K. W. Stone, D. B. Turner, and K. A. Nelson, "Multidimensional coherent spectroscopy made easy," Chem. Phys. **341**, 89 – 94 (2007).
21. U. Selig, F. Langhojer, F. Dimler, T. Löhrig, C. Schwarz, B. Gieseking, and T. Brixner, "Inherently phase-stable coherent two-dimensional spectroscopy using only conventional optics," Opt. Lett. **33**, 2851–2853 (2008).
22. M. J. Nee, R. McCanne, K. J. Kubarych, and M. Joffre, "Two-dimensional infrared spectroscopy detected by chirped pulse upconversion," Opt. Lett. **32**, 713–715 (2007).
23. L. Lepetit, G. Chériaux, and M. Joffre, "Linear techniques of phase measurement by femtosecond spectral interferometry for applications in spectroscopy," J. Opt. Soc. Am. B **12**, 2467–2474 (1995).
24. K. F. Lee, K. J. Kubarych, A. Bonvalet, and M. Joffre, "Characterization of mid-infrared femtosecond pulses," J. Opt. Soc. Am. B **25**, A54–A62 (2008).

1. Introduction

Interferometers have a long and interesting history due to their ability to control optical paths on the nanometer scale [1,2]. We are interested in midinfrared (midIR) multidimensional spectroscopy, which requires subwavelength knowledge of the path difference between two arms of an interferometer, since the measured signal oscillates on the scale of the wavelength of the pulses being delayed [3]. To meet this requirement, we have developed a method that can measure path delays without adding optical elements that might affect the midIR beam, by periodically modulating the path length of one arm.

In a conventional interferometer, a retroreflecting mirror moves with a translation stage, changing the path length of one arm. The simplest path measurement is to reference the rotation of the stage's driving screw against a physical ruler. This is generally not precise enough, if only because backlash adds a shift between forwards and backwards measurements. Advanced stages can have very precise physical rulers along the length of the stage. However, the position of the stage itself is not the same as the mirror which is mounted above the stage, and the stage position does not include vibrations of the other optics in the interferometer.

To measure the full path delay, one can try to use the existing laser beam, or add a continuous wave laser beam that copropagates with the original beam to aid tracking. Tracking beams are particularly useful for pulsed and infrared beams, since they are harder to work with. A tracking beam, after traveling through the interferometer, will give a spot that changes from bright to dark as the changing path delay changes the relative phase of the two electric fields. This flashing indicates a path delay change, but not the direction of the change. Thus, one approach is to track the interferometer only while it is moving in a known direction, either by scanning [4], or actively locking the delay [5,6] and stepping the delay by fractions of the wavelength [7].

We would like to continuously scan, while recording a spectrum and path delay for each laser shot. To continuously track, we need to generate the quadrature of the oscillating signal, that is, a complementary signal that is $\pi/2$ radians out of phase with the photodiode signal. Together, the two quadratures describe both the position and direction of motion, allowing continuous tracking.

One approach to generating the other quadrature is to use waveplates and polarizers to create two shifted polarizations [8-11], but this requires adding a waveplate to the infrared beam path. One way to avoid this problem is to reflect the tracking beam from the backside of the delay stage [12]. While sufficient in some cases, this will only measure the stage, not the complete path delay. Another approach is to combine the beams from the two arms at an angle, so that there is an array of light and dark lines rather than a single spot [13,14]. The

#111806 - $15.00 USD Received 26 May 2009; revised 24 Jun 2009; accepted 1 Jul 2009; published 7 Jul 2009

light and dark portions can be measured by a detector array [15,16], providing both quadratures. The required angle between the beams means that this method is suited for cases where the beams are combined at an angle, rather than beams that copropagate after recombination.

In the method we present here, we generate the other quadrature by mounting a mirror in one interferometer arm on a piezoelectric stack to oscillate the path length of that arm. To understand the process, we first imagine an interferometer that is completely stable. The photodiode reports a voltage that we take to be one quadrature. If we then change the path delay by $\lambda/4$ with the piezo, the photodiode will now give the second quadrature. In a moving interferometer, if the piezo is moved quickly relative to the interferometer motion, this view is approximately correct, and one can measure the signal and quadrature by recording the diode signal as the piezo oscillates. We work here with collinear beam geometries, but we have also used a noncollinear beam geometry by selecting out one part of the fringe pattern with a slit.

Besides measuring the path delay of an interferometer, other beam control methods have been developed for multidimensional spectroscopy. These involve enforcing a given path length by using single optical elements such as diffractive optics [17,18], pulse shapers [19,20], or particular optical arrangements that are passively stable [21]. These methods have their particular limitations and benefits, such as limited bandwidth, or better ease of operation. In our particular case, we have chosen to use interferometers, which requires path delay measurements. By oscillating the optical path length, we are able to measure the path delay of our interferometers with few-nm accuracy without adding any optical elements to the beam path.

2. Experimental

We track a Michelson-Morley interferometer [1] for 800 nm pulses, and a Mach-Zehnder interferometer, similar to Fig. 1, for midIR pulses. For the tracking beam, we use a helium-neon (HeNe) laser, chosen for its wavelength stability, narrow linewidth, and simplicity. The midIR pulses are the difference frequency of the signal and idler of an optical parametric amplifier driven by the same Ti:Sapphire regenerative amplifier producing the 800 nm pulses. We detect the midIR by chirped pulse upconversion to visible light, and a CCD imaging spectrometer [22].

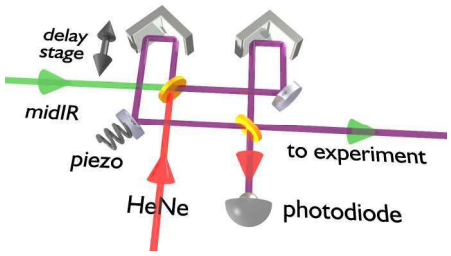

Fig. 1. Illustration of a midinfrared interferometer with HeNe tracking by path length oscillation. Other than the piezo, the interferometer is unchanged when adding tracking.

We used optics specified for the pulsed beam wavelengths, ignoring the tracking beams. Extra tracking beams from surface reflections can make alignment more difficult, but tracking functions normally. Using a lens to focus on the photodiode can help separate extra reflections from wedged optics. The only added optic was a calcium fluoride window before the infrared interferometer for coupling the tracking beam to the infrared beam, although this can be avoided by using the other entrance port of the beam splitter as in Fig. 1. This is the case for the 800 nm interferometer, where the beam is coupled in through the other exit port.

To oscillate the path length, a mirror in one arm is mounted on a piezoelectric stack. The piezo is calibrated by adjusting until the Lissajous figure, where the x and y components are the photodiode signal and the derived quadrature, becomes circular. One signal generator synchronously controls the piezo motion with a sinusoid at 2 kHz, the regenerative amplifier

#111806 - $15.00 USD Received 26 May 2009; revised 24 Jun 2009; accepted 1 Jul 2009; published 7 Jul 2009

and CCD at 1 kHz, and the photodiode acquisition at 32 kHz. Since the piezo is at a multiple of the laser frequency, the mirror returns to the same point at each laser shot, allowing large or complex piezo motion. Synchronizing the piezo and photodiode to the laser is not strictly necessary, but it improves accuracy by minimizing the time delay between the laser pulses and the photodiode. The photodiode signals are recorded by a computer, analyzed, and the path delays for each laser shot are saved synchronously with the spectrum for each pulse.

3. Calculation

From the oscillating photodiode signal of the interfering HeNe beams, we can calculate the quadrature, knowing that the piezo is imposing a path length oscillation of $\pi/2$ radians, or a quarter of the HeNe wavelength, and assuming that the motion of the interferometer is small relative to the piezo motion, which is usually true. If we take the first data point to be at the top of the hill of the piezo oscillation, as shown on the left of Fig. 2, we can immediately say that the next valley of the oscillation is the corresponding quadrature, due to the chosen $\pi/2$ delay from the piezo. One might notice that the valley backwards in time is equivalent. When the interferometer is moving linearly, one valley point will have an extra forward displacement, and the other value will have an extra backwards displacement. By averaging the forward and backward valleys, the linear component of the motion is reduced, better approximating the actual quadrature value. Working in the complex plane, the photodiode signal, scaled between -1 and 1, is the real component, and the extrapolated quadrature is the imaginary component. When well calibrated, the points will move on the unit circle as the delay changes, with the phase angle corresponding to the relative HeNe phase, as in the right plots of Fig. 2.

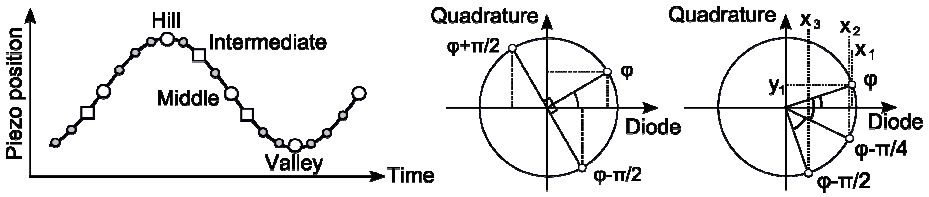

Fig. 2. On the left is a schematic of the piezo oscillation in time. Points on the curve indicate acquisition times. Hollow circles and squares show two groupings for calculating quadratures. The two plots on the right show data points in complex space. The real component is the scaled diode measurement. The imaginary component is the calculated quadrature.

We can now track the interferometer, but at only 2 kHz, the tracking would be lost during vibrations if the difference between measurements exceeded π. To maintain tracking, we want quadratures for each of the 16 points per piezo cycle. For valley points, the quadrature can be found using adjacent hills, noting that the piezo moves in the opposite direction to the hill case. In the middle plot of Fig. 2, if φ is a hill point, the valley would be the point $\varphi - \pi/2$, whose diode reading would be the quadrature value. If φ is a valley, moving to a hill would be going the other way, to $\varphi + \pi/2$. Removing the π offset by multiplying by -1 gives the desired quadrature.

The middle points have adjacent valley and hill points that are offset by $\pi/4$. Looking at the right plot of Fig. 2, we have the middle point measurement, $x_1 = \cos(\varphi)$, and the next valley, $x_2 = \cos(\varphi - \pi/4)$. We extrapolate the desired quadrature $y_1 = x_3 = \cos(\varphi - \pi/2)$, using the trigonometric formula: $\cos(\alpha - \beta) = 2\cos(\alpha)\cos(\beta) - \cos(\alpha + \beta)$. With $\alpha = \varphi - \pi/4$, and $\beta = \pi/4$, we get $x_3 = 2^{1/2}x_2 - x_1$. We also average the adjacent valley and hill contributions. For consistency, we apply this same $\pi/4$ extrapolation to the hill and valley calculations, using their adjacent middle points. This reduces the time range, and thus sensitivity to fast motion.

For the intermediate points, we also look for points offset by $\pi/4$, but the forward and backward points that are averaged are no longer symmetric in time. Consider the second point just after the hill, shown as a square on the left of Fig. 2. The square three points forward in time, is offset by approximately $\pi/4$. However, going three points back in time gives the wrong offset, so we go seven points back, matching the forward point. The

#111806 - $15.00 USD Received 26 May 2009; revised 24 Jun 2009; accepted 1 Jul 2009; published 7 Jul 2009

asymmetry means that the averaging removes less of the linear motion. Since our laser shots are synchronized to every other hill point, small errors in intermediate points do not affect the experiment, since they only maintain tracking between laser pulses.

4. Testing

To test our tracking system, we simultaneously measured the position of the 800 nm interferometer by HeNe, and by recording the spectral fringes from the interfering 800 nm pulses with the CCD spectrometer. The Ti:Sapphire spectrum is analogous to the HeNe photodiode signal, but multiplexed over hundreds of pixels for different wavelengths. Fourier analysis of these spectra to extract the analytic signal [23,24] yields precise information about the path delay for each laser shot.

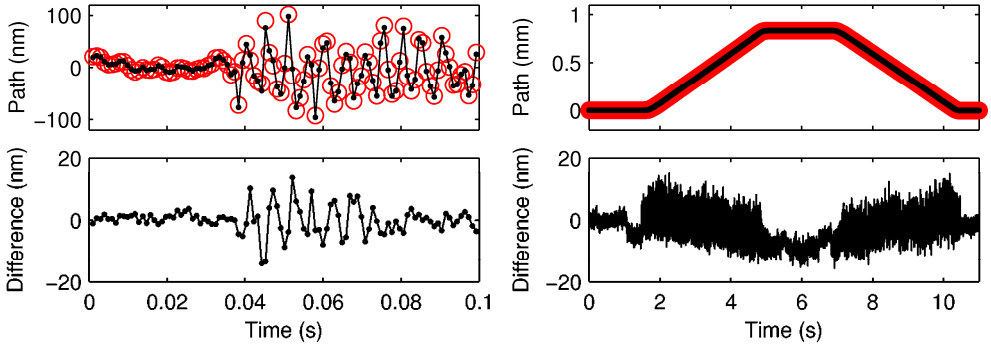

Fig. 3. The upper plots show the optical path delay as measured by the Ti:Sapphire fringes (small points on left, small line on right), and HeNe tracking (large points on left, large line on right). The lower plots show the difference between the two measurements. The plots on the left correspond to tapping of the optical table. The plots on the right correspond to scanning of the delay by motor. The two measurement types agree to within 20 nm.

The upper left plot of Fig. 3 shows the path delay with time when the optical table is tapped. When undisturbed, the HeNe and Ti:Sapphire measurements agree to within a few nanometers. The tapping induces vibrations in the interferometer, and also increases the difference between the measurements to about 20 nm as seen in the lower left plot. High speeds and acceleration cause visible ellipticity of the Lissajous figure as effects from the low speed approximation, imperfect piezo calibration, and small differences between HeNe and Ti:Sapphire signal acquisition times, become more pronounced.

A similar test is shown on the right of Fig. 3. Here, the delay in one arm is scanned by motor. As before, the difference between the HeNe and Ti:Sapphire measurements increases when the arms are moving, but still remains within 20 nm. The linear change in the difference as the motor moves is a calibration error between the HeNe and Ti:Sapphire measurements, likely due to a small angle between the HeNe and Ti:Sapphire beams. The calibration can be corrected with this type of data. The wavelength calibration can play a part as well; the HeNe wavelength was not directly measured, and the 800 nm spectrum was calibrated using lines from a krypton lamp, but these errors are expected to be very small.

Since we are interested in multidimensional spectroscopy, we took a two-dimensional (2D) spectrum of human carboxy-hemoglobin (HbCO) in a D_2O Tris-HCl buffer, while tracking with both the HeNe, and the rotary encoder on the DC motor driving the stage. The 2D spectrum is taken using the pump-probe geometry [4,19], scanning the time delay between two midIR pump pulses with the interferometer. The 2D spectrum is made by Fourier transform against this time delay. Data was acquired for each laser shot as the motor continuously drove the stage.

For this comparison, only one scan direction was used to avoid backlash effects in the encoder data. Laser noise was reduced by normalizing the area of each spectrum. Since tracking lets us scan continuously, the scan maps noise from actual time to path delay. By

#111806 - $15.00 USD Received 26 May 2009; revised 24 Jun 2009; accepted 1 Jul 2009; published 7 Jul 2009

scanning quickly enough, noise will modulate the data more slowly than the actual signal. After the Fourier transform, the noise will appear at low frequencies, separated in Fourier space from the higher frequency signal of interest. Mechanical chopping for removing laser noise is thus unnecessary, greatly benefitting acquisition rate. If conventional chopping were used, position interpolation would be needed while the tracking beam was blocked.

Multiple scans are averaged by fractional binning by time delay. Two adjacent bins receive a fraction of each spectrum. For example, for one spectrum at a time delay of 1.3 fs, and with 1 fs bin spacing, 70% of the counts would be added to the 1 fs bin, and 30% to the 2 fs bin. These count as 70% and 30% of a spectrum when the bin is divided by the number of spectra per bin.

Figure 4 shows the measured 2D spectra. The spectrum on the left uses the path delay reported by the motor encoder for the Fourier transform. The spectrum on the right uses the path delay found by HeNe tracking. The encoder spectrum is smeared along the transformed axis due to the inconsistent motor reading. With HeNe tracking, the expected peaks from the CO vibration, and sample-independent effects along the diagonal from the interference of scattered light [19] become readily apparent.

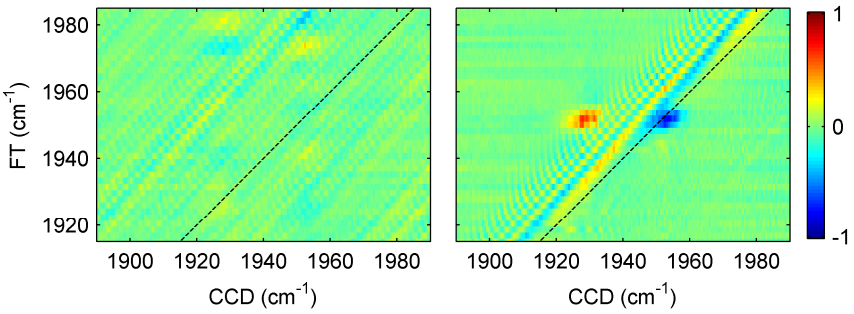

Fig. 4. A color map of the real part of the 2D midIR spectrum of HbCO. The left spectrum was made with position information from the motor encoder. The spectrum on the right uses positions reported by HeNe tracking. The motor encoder is sufficiently inaccurate that the 2D spectrum vanishes. The axes labeled CCD are the measured wavelengths from the spectrometer, and the FT axes are obtained by Fourier transformation of the scanned time delay. The dashed lines indicate the location of the diagonal.

5. Conclusion

We can track interferometer path delays with few-nanometer precision by path length oscillation. When exposed to vibrations, the tracking is maintained to within less than 20 nm. Since 20 nm is λ/250 for a 5 μm beam, this precision is sufficient for our application of midIR multidimensional spectroscopy. For more demanding applications, faster acquisition rates and better calibration can increase precision and stability against vibrations.

Our method has the advantages that it is accurate, introduces no additional optical elements to the beam path, includes the entire path of both arms, and functions for both collinear and noncollinear beam recombination geometries. While we use continuous scanning, this method can also be used to lock the interferometer, but without being limited to simple fractions of the HeNe wavelength. In addition to multidimensional spectroscopy, this is a flexible method that may be useful in many other applications.

Acknowledgements

We acknowledge Xavier Solinas for electronics support, and Agence Nationale de la Recherche (ANR-BLAN-0286) for financial support. PN acknowledges Deutsche Akademie der Naturforscher Leopoldina (BMBF-LPDS 2009-6) for financial support.

#111806 - $15.00 USD Received 26 May 2009; revised 24 Jun 2009; accepted 1 Jul 2009; published 7 Jul 2009